

See discussions, stats, and author profiles for this publication at: <https://www.researchgate.net/publication/5405857>

ChemInform Abstract: Photocontrol of Neural Activity: Biophysical Mechanisms and Performance in vivo

ARTICLE *in* CHEMICAL REVIEWS · JUNE 2008

Impact Factor: 46.57 · DOI: 10.1021/cr078221b · Source: PubMed

CITATIONS

42

READS

42

2 AUTHORS, INCLUDING:



Lucas Sjulson

New York University

12 PUBLICATIONS 773 CITATIONS

SEE PROFILE

Photocontrol of Neural Activity: Biophysical Mechanisms and Performance *in Vivo*

Lucas Sjulson[†] and Gero Miesenböck^{*,‡}

Department of Cell Biology, Yale University School of Medicine, 333 Cedar Street, New Haven, Connecticut 06520, and Department of Physiology, Anatomy and Genetics, University of Oxford, Sherrington Building, Parks Road, Oxford OX1 3PT, United Kingdom

Received February 11, 2008

Contents

1. Introduction	1588
2. Photoablation and Photoinactivation	1589
2.1. Dye-Mediated Photoablation of Cellular Targets	1589
2.2. Genetically Targeted Small Molecule Photoablation of Cellular Targets	1589
2.3. Chromophore-Assisted Light Inactivation (CALI) of Molecular Targets	1590
2.4. KillerRed	1591
3. Photomanipulation of Membrane Potential	1591
3.1. The Role of Ion-Selective Conductances	1591
3.2. The Effect of Background Synaptic Activity: Low- and High-Conductance States	1592
3.3. Thermal Photostimulation	1593
3.4. Reactive Oxygen Species-Mediated Photostimulation	1593
3.5. Caged Glutamate	1594
3.6. Caged GABA	1594
3.7. Genetically Encoded Photomodulators of Membrane Potential	1595
3.7.1. Rhodopsins	1595
3.7.2. Proteins Regulated via Exogenous Light-Sensitive Molecules	1598
4. Conclusion	1600
5. Acknowledgments	1601
6. References	1601

1. Introduction

Nervous systems run on electricity. Information is represented as differences in electric potential and processed by active devices—nerve cells—that generate stereotyped output signals (action potentials or spikes) in response to variation in input potential. Like most bioelectric potentials, the electrical signals of neurons are diffusion potentials; they are established by ionic concentration gradients across the external neuronal membrane and controlled by different types of ion-selective conductances (see section 3.1). Some of these conductances (voltage-gated ion channels) are regulated locally, by virtue of their ability to sense the electric potential across the membrane in which they sit, whereas others respond to chemicals (neurotransmitters) that report potential changes in distant, synaptically connected cells. Loosely

speaking, the interplay of local membrane potential differences, electrotonic currents driven by these differences, and voltage-gated conductances defines the information-processing capabilities of a single neuron.

Neurons, however, do not operate in isolation. They are embedded into circuits of often staggering complexity in which each cell is influenced by, and influences, many others via thousands of afferent and efferent synaptic connections. This multitude of interactions supports a vast array of biophysical phenomena that allow circuits to perform functions that would be impossible to implement with single cells. Unfortunately, however, the distributed nature of neural circuits also makes them exceedingly difficult objects for experimental study: the standard approach of recording the electrical activity of a single neuron is often inadequate for understanding the function of a circuit. Optical methods are potentially better matched than electrodes to the distributed information-processing architecture of the nervous system.^{1–4} Optical recording of voltage-controlled ionic fluxes or cell-to-cell communication, for example, can reveal the dynamics of signaling in entire populations of neurons with cellular or synaptic resolution.^{5–7}

Yet a full arsenal of experimental tools for studying the nervous system must include techniques to manipulate neural activity as well as record it. Aside from patterned sensory stimulation, the most common methods for controlling neuronal signaling have been lesioning, pharmacology, and electrical stimulation. Only in recent years have optical methods also begun to have a significant impact in this domain. This trend is due, in large part, to three advantages. The first is the excellent spatial and temporal resolution of many optical approaches. The second is the ability to control neural activity in a “hands-off” manner, which allows probing of many tissue sites simultaneously or in rapid succession. The third, and most recent, advantage arises when a pinch of genetics is added to the optical mix; neuronal activity can then be recorded and manipulated with “genetic resolution”.^{3,4,8} By encoding an optically responsive protein in DNA and using cell-type specific promoters or localized DNA delivery to control expression, photosensitivity can be restricted to a subset of cells in a given anatomical region, based on the cells’ functional identity or connectivity, rather than just their location.

The power of genetically targeted photomanipulation was foreseen by Francis Crick, who in his 1999 Kuffler Lectures raised the “far-fetched” possibility that molecular biologists could “engineer a particular cell type to be sensitive to light”.⁹ But such foresight was by no means universal. When the first experiments realizing Crick’s vision were submitted

* To whom correspondence should be addressed. E-mail: gero.miesenboeck@dpag.ox.ac.uk.

[†] Yale University School of Medicine.

[‡] University of Oxford.



Luke Sjulson was born in Crookston, Minnesota in 1977. He received his B.A. in Neuroscience from Johns Hopkins University in 1999 and his Ph.D. in Neuroscience with Gero Miesenböck (at Yale University) through the Cornell/Rockefeller/Sloan-Kettering Tri-Institutional MD/PhD Program in 2007. After completing his MD in 2008, he will begin psychiatry residency training at NYU Medical Center. His research interests involve studying abnormal brain dynamics in animal models of psychiatric disease using combinations of optical, molecular, electrophysiological, and computational approaches.



Gero Miesenböck is the Waynflete Professor of Physiology at the University of Oxford and a Fellow of Magdalen College. He was born and educated in Austria, where he completed his MD at the University of Innsbruck in 1993. Before moving to Oxford in 2007, he spent more than a decade in the United States, holding faculty appointments at Memorial Sloan-Kettering Cancer Center and Yale University. Miesenböck is a principal architect of genetic strategies for observing and controlling neural activity with light. He uses these optical approaches to read and change the minds of fruit flies; his current research focuses on the structure and dynamics of circuits involved in sensory processing, action selection, and motor pattern generation.

for publication,⁸ an anonymous referee questioned what would be gained by expressing optically controlled actuators of neural activity in cells of the hippocampus, a phylogenetically old part of the cerebral cortex: would it not be easier to study the retina instead, which “conveniently has light-sensitive cells already built in?”

Over the past six years, such narrow-minded resistance has been buried under a veritable avalanche of work with light-controlled actuators, driven by expanding technical developments^{8,10–16} and novel applications to the analysis of neural circuitry^{17–19} and behavior.^{20–27} This review discusses the various photomanipulation technologies that have been demonstrated in the nervous system, with an emphasis on the underlying biophysical mechanisms and the performance limits they impose.

2. Photoablation and Photoinactivation

There are two general methods for controlling neural activity with light: photoablation and photomanipulation of membrane potential. Photoablation, or killing a subset of cells by illumination, is conceptually simpler and often advantageous when fast onset and long duration of action are required but reversibility is not. With sufficient light intensity, it is possible to photoablate any cell through local heating or permeabilization of the membrane;²⁸ however, almost all methods for photoablation of specific sets of cells are based on the principle of chromophore photoexcitation producing reactive oxygen species (ROS), which in turn leads to cell death.²⁹

2.1. Dye-Mediated Photoablation of Cellular Targets

This class of techniques involves loading subsets of neurons with a small-molecule dye, which photosensitizes those cells by increasing the efficiency of light-induced ROS generation. The first demonstration of this technology involved loading dye into cells through an intracellular electrode³⁰ (Figure 1A), though later versions relied on less laborious nonspecific uptake³¹ or even specific axonal uptake,³² which permits photoablation based on anatomic projection patterns. Despite the lack of genetic resolution, these techniques have been used in several systems with great success, particularly marine invertebrates.^{33,34}

2.2. Genetically Targeted Small Molecule Photoablation of Cellular Targets

The first genetically targeted photoablation method utilized cell-type specific expression of the *E. coli* lacZ gene,³⁵ which encodes β -galactosidase (β -gal), a bacterial enzyme that hydrolyzes glycosidic bonds (Figure 1B). A nonfluorescent fluorescein analog, fluorescein-di- β -D-galactopyranoside (FDG, **1**), is added to the bath solution and taken up into cells, where β -gal then converts the FDG, **1** to fluorescein, **2** (Figure 2), driving its selective accumulation in β -gal-expressing cells.³⁵ Since fluorescein alone is a rather poor sensitizing agent in these circumstances, the efficiency of this process was improved substantially by the addition of a nontoxic reducing agent, 3-amino-ethylcarbazole, **3** (Figure 3), which converts to a toxic product when oxidized. This method has been shown to enable efficient cell-type specific ablation *in vitro*; however, general applications *in vivo* are likely limited to superficial structures, because most tissues impede the penetration of FDG and 3-amino-ethylcarbazole and are opaque to the blue wavelengths used to excite fluorescein. Indeed, this technology has proven particularly powerful in the study of the intrinsic circuitry of the thin and optically transparent retina, in which ablation of various genetically defined amacrine cell subtypes has been shown to affect the duration³⁶ and spatial frequency tuning³⁷ of retinal ganglion cell responses.

Although other methods have been developed to target accumulation of fluorescent small molecules to genetically defined subpopulations of cells, none of these have been explicitly tested for the purpose of photoablation. For example, β -lactamase has been used to convert several nonfluorescent molecules to fluorescent dyes,³⁸ analogous to the conversion of FDG to fluorescein by β -gal.³⁵ Overexpression of the uroporphyrinogen III methyltransferase

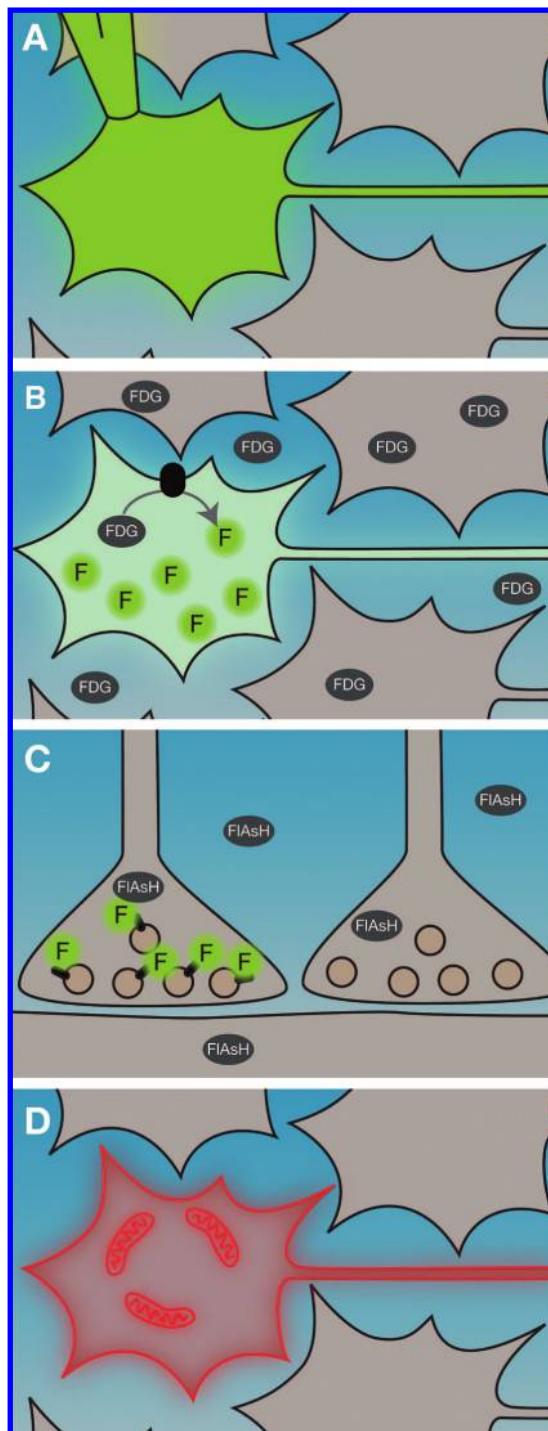


Figure 1. Photoablation of cellular and molecular targets: (A) loading of single neurons with a fluorescent photosensitizer through a patch pipet; (B) β -galactosidase expression in genetically defined subpopulations of neurons converts nonfluorescent FDG to fluorescein (F), a photosensitizing agent; (C) CALI, selective inactivation of proteins decorated with a sensitizing chromophore (F); (D) targeted expression of KillerRed in mitochondria or at the plasma membrane enables photoablation of genetically defined cell populations.

gene leads to cytoplasmic accumulation of the small molecule fluorophores sirohydrochlorin, **4**, and trimethylpyrrocorphin, **5** (Figure 4), without addition of exogenous cofactors.³⁹ The efficiency of this process can be increased significantly by the addition of 5-aminolevulinic acid,⁴⁰ **6**, a relatively nontoxic intermediate in porphyrin biosynthesis known to cross the blood–brain barrier from the circulation.⁴¹ If these

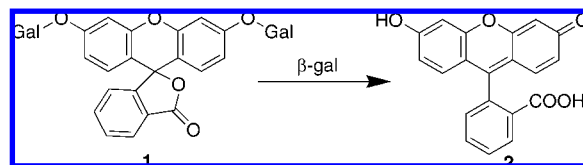


Figure 2. Conversion of FDG to fluorescein by β -galactosidase.

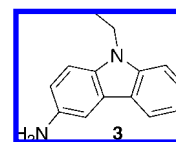


Figure 3. 3-Amino-ethylcarbazole.

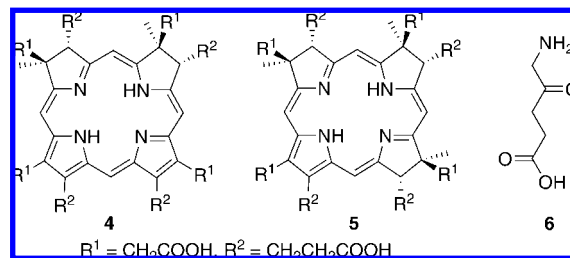


Figure 4. Porphyrins and 5-aminolevulinic acid,

molecules prove to produce sufficient ROS for photoablation, the simplified requirements for exogenous cofactors could greatly improve the applicability of this method *in vivo*.

2.3. Chromophore-Assisted Light Inactivation (CALI) of Molecular Targets

Rather than filling an entire cell diffusely with a sensitizing chromophore, the destructive power of ROS can be localized more precisely by attaching the photosensitizer to a specified molecular target⁴² (Figure 1C). This approach was termed chromophore-assisted light inactivation (CALI), a fitting allusion to Kali, the goddess of doomsday and death in Hinduism. The initial incarnation of CALI involved the delivery of malachite green (MG)-derivatized affinity reagents (generally antibodies) that are directed against the targets of inactivation.⁴² Laser irradiation at high intensity then damaged these targets irreversibly, provided they were held within ~ 60 Å of the MG chromophore.⁴³ It was subsequently found that substituting fluorescein (**2**) for MG results in >50 -fold higher inactivation efficiencies;⁴⁴ this reincarnation of CALI has become known as fluorophore-assisted light inactivation (FALI).⁴⁵

A serious obstacle to the widespread application of CALI and FALI has been their dependence on bulky, membrane-impermeant sensitizing agents, typically dye-conjugated antibodies or antibody fragments,^{42–45} that must be injected into the cells of interest. The development of membrane-permeant fluorescein derivatives^{46,47} that selectively bind to small receptor domains in proteins⁴⁶ offers a potential route around this problem. The receptor domains contain the sequence -Cys-Cys-Pro-Gly-Cys-Cys-, which forms a hairpin structure⁴⁷ in which the spacing of the two thiol pairs matches that of two As(III) substituents in the complementary 4',5'-bis(1,3,2-dithioarsolan-2-yl)fluorescein ligand (FIAsH).⁴⁶ Importantly, FIAsH is virtually nonfluorescent when bound to small-molecule dithiol antidotes such as 1,2-ethanedithiol (EDT, **7**) but increases its quantum yield by more than 4

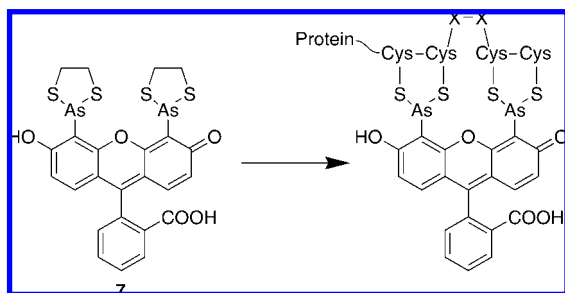


Figure 5. FIAsh bound to 1,2-ethanedithiols (EDT₂) and a tetracysteine-containing polypeptide.

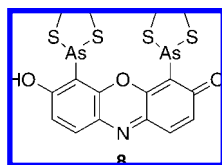


Figure 6. ReAsH bound to 1,2-ethanedithiols (EDT₂).

orders of magnitude when the EDTs are exchanged for a more rigid and constrained tetracysteine peptide⁴⁷ (Figure 5).

Insertion of the tetracysteine motif into synaptotagmin I, a synaptic vesicle protein thought to function in Ca²⁺-dependent neurotransmission, has permitted the acute and selective optical inactivation of this protein in *Drosophila* larvae.⁴⁸ Consistent with a role of synaptotagmin I in sensing the Ca²⁺ signal for exocytosis, illumination of the larval neuromuscular junction caused an acute block in evoked, Ca²⁺-dependent transmitter release but left spontaneous, Ca²⁺-independent vesicle release unaffected. Despite this successful proof of principle,⁴⁸ the contrast between FIAsh labeling of the intended molecular targets and background staining often remains poor, creating a need for optimized biarsenical-binding tetracysteine motifs or chromophores.^{47,49} For example, substituting the red biarsenical dye, ReAsH, **8** (Figure 6),⁴⁷ for FIAsh was found to reduce substantially the light doses required for inactivating connexin43, a major component of gap junctions.⁵⁰ Irrespective of chromophore choice, however, genetically targeted CALI can aim only at tetracysteine-tagged proteins and not their endogenous counterparts and may therefore require disruption of endogenous gene expression to be effective.

2.4. KillerRed

Another strategy to facilitate genetically encoded photoablation of cellular or molecular targets would be to eliminate the requirement for exogenous cofactors altogether by using variants or homologues of green fluorescent protein (GFP) as photosensitizers. GFP is not ideally suited for this role, because its chromophore is shielded by a β -barrel shell, which limits access to molecular oxygen and thus prevents the efficient generation of ROS. Part of GFP's success in fluorescence microscopy is precisely due to its low phototoxicity. Nevertheless, relatively inefficient photoablation of cells expressing mitochondrially targeted GFP has been demonstrated.⁵¹ Recently a dimeric red fluorescent protein named KillerRed was introduced that generates ROS over 1000 times more efficiently than GFP,⁵² in a range comparable to some small molecule dyes. When KillerRed is targeted to the mitochondria or the plasma membrane (Figure 1D), several minutes of illumination causes irreversible cell death tens of minutes later. KillerRed can also be fused

directly to proteins of interest, enabling CALI without exogenous cofactors;^{52,53} however, KillerRed is dimeric and may cause some proteins to aggregate.

Despite the promise of these photoablation technologies, there have been no studies demonstrating their effectiveness in the intact mammalian CNS. Oxygen tension is higher *in vivo*, which should facilitate the generation of ROS; however, mammalian plasma membranes are protected by the bilirubin–biliverdin reductase antioxidant system,⁵⁴ which may render cells resistant to ROS-mediated photoablation. Although this antioxidant system can be disrupted pharmacologically,⁵⁵ the efficiency of cellular photoablation technologies in the intact mammalian brain remains unknown.

3. Photomanipulation of Membrane Potential

The more generally applicable method for photocontrol of neural activity is photomanipulation of membrane potential, which possesses onset and reversibility on very fast time scales and affords a superior degree of experimental control, including the capacity to probe the function of neural systems inside and outside their normal physiological limits.^{4,25} In many situations, the temporally and spatially controlled induction of neural activity will prove more informative than the ablation or silencing of neurons, where generation of phenotypes depends on disruption of activity that is either present at baseline or evoked by sensory stimuli or behavioral tasks.

3.1. The Role of Ion-Selective Conductances

The neuronal membrane potential is a direct consequence of transmembrane ionic concentration gradients and selective ionic permeability through ion channels. A given ionic population X is associated with an equilibrium potential, E_X , at which there is zero net current flow for that ion. The Nernst equation determines this potential as a function of ionic concentration on each side of the membrane:

$$E_X = \frac{RT}{zF} \ln \frac{[X]_o}{[X]_i} \quad (1)$$

where R is the gas constant, T is the temperature, z is the valence of the ion, F is Faraday's constant, and $[X]_o$ and $[X]_i$ are the concentrations of ion X on the outside and inside of the cell, respectively. Neuronal membrane potentials are dominated by the ionic conductances for sodium, potassium, and chloride; typical values for the equilibrium potentials of these ions in mammalian neurons are $E_K = -90$ mV, $E_{Cl} = -75$ mV, and $E_{Na} = +55$ mV. The membrane potential of a passive membrane compartment at equilibrium can be approximated by an average of the equilibrium potentials of the ionic species present, weighted by their relative conductances g_X , with an additional contribution from nonselective synaptic conductances (g_{syn} , with $E_{syn} = 0$ mV):

$$V_m \approx \frac{g_{Na}E_{Na} + g_K E_K + g_{Cl} E_{Cl} + g_{syn} E_{syn}}{g_{Na} + g_K + g_{Cl} + g_{syn}} \quad (2)$$

Of course, real neurons do not have passive membranes; while eq 2 is useful for understanding the effects of photomodulating ion-selective conductances, Figure 7 depicts the effect of altering various ionic conductances on firing patterns in a more realistic model of neuronal membrane potential.⁵⁶ Equation 2, however, captures the main concep-

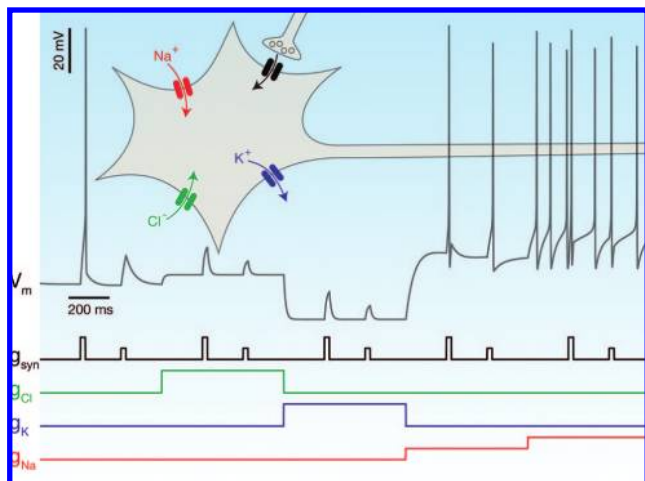


Figure 7. Effect of ionic conductances on firing patterns. Transmembrane voltage changes in this model cell (gray trace) are driven by pulsed synaptic inputs (black trace). The model shows the cell's responses to five consecutive pairs of synaptic impulses. Under physiological conditions (left), strong synaptic inputs elicit action potential firing, but weak synaptic inputs remain subthreshold. Increasing Cl^- conductance (green) decreases responsiveness to synaptic inputs through "shunting inhibition" (see text). Increasing K^+ conductance (blue) hyperpolarizes the cell, overriding synaptic inputs. Increasing Na^+ conductance (red) either drives subthreshold inputs over the firing threshold or directly elicits action potential firing.

tual point, which is that increasing a given membrane conductance pulls the membrane potential closer to the equilibrium potential associated with that conductance. For example, opening K^+ -selective channels, thereby increasing g_{K} , draws the membrane potential closer to E_{K} ; this "hyperpolarizes" the membrane and prevents action potential firing (blue trace, Figure 7). On the other hand, increasing g_{Na} by opening ideal Na^+ -selective channels pulls the membrane potential toward E_{Na} , thereby "depolarizing" the membrane and pushing subthreshold inputs over the firing threshold or even eliciting action potentials directly (red trace, Figure 7). Real Na^+ channels, however, are only partially selective for Na^+ over other cations, and therefore pull the membrane potential instead toward their "reversal potential," which is an average of the equilibrium potentials of the permeant ions weighted by their permeability through the channel. Nevertheless, the effect on firing patterns is qualitatively similar, as it is for Ca^{2+} -selective or nonselective cation channels, both of which possess reversal potentials above the threshold for action potential firing.

Cl^- -selective conductances are more complex. Since E_{Cl} is generally close to the resting membrane potential, opening Cl^- channels and increasing g_{Cl} may or may not lead to a significant change in membrane potential, depending on the membrane potential and value of E_{Cl} in that particular cell. However, opening any conductance decreases the cell's input resistance, which is the voltage change caused by current injection—for example, by activating a synaptic input—into the cell divided by the amount of current injected. In other words, an increased Cl^- conductance (green trace, Figure 7) may even depolarize the membrane slightly but render the cell resistant to further depolarization from synaptic conductances (g_{syn} , black line, Figure 7). This is called "shunting inhibition," and can also be understood as an increase in the denominator in eq 2, which decreases the relative impact of the synaptic term ($g_{\text{syn}}E_{\text{syn}}$) on overall membrane potential.

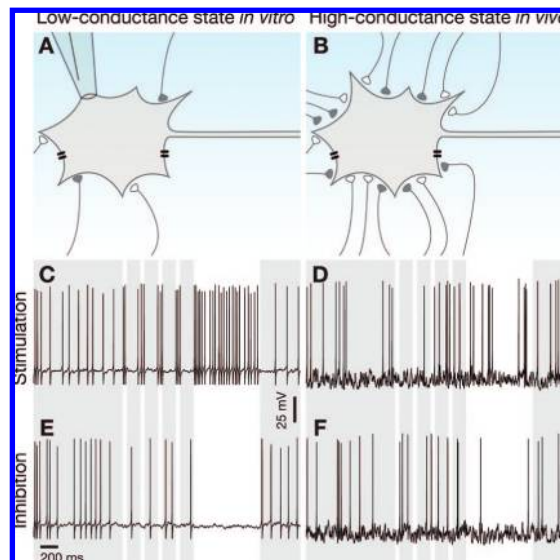


Figure 8. Low- and high-conductance states: (A) A cell in the low-conductance state *in vitro*, characterized by a small number of active synaptic inputs, high input resistance, and stable resting membrane potential; (B) a cell in the high-conductance state *in vivo*, characterized by a large number of active synaptic inputs, low input resistance, and a highly variable resting membrane potential; (C) under low-conductance conditions, 200 pA depolarizing current pulses (white background) reliably elicit action potentials; (D) under high-conductance conditions, 200 pA depolarizing current pulses (white background) tend to increase mean firing rate but are unable to elicit firing reliably; (E) under low-conductance conditions, 200 pA hyperpolarizing current pulses (white background) reliably inhibit action potential firing; (F) under high-conductance conditions, 200 pA hyperpolarizing current pulses (white background) tend to decrease mean firing rate but are unable to prevent action potential firing.

Ion-selective conductances thus create and control the cellular membrane potential, and the methods for photomanipulation of membrane potential that we discuss generally act on ion channels, either by modulating existing channels or by adding new channels that can be controlled with light.

3.2. The Effect of Background Synaptic Activity: Low- and High-Conductance States

Not all changes in ionic conductances lead to reliable control of neural activity, however; the amplitude of the induced conductance must be sufficient to override synaptic inputs and other endogenous currents. The conductance required to induce or prevent spiking depends not only on the size and type of cell, but also on the strength and variability of synaptic input. For example, neurons in culture or tissue slices, or even in anesthetized animals, have a small number of active synaptic inputs relative to cells in the brains of awake behaving mammals (Figure 8A,B). As a result, cells *in vitro* reside in a "low-conductance state" characterized by low membrane potential variability and high input resistance. In this state, small injections of current are sufficient to cause large changes in membrane potential. Cortical neurons in waking animals, in contrast, are subject to a constant barrage of synaptic impulses, leading to a "high-conductance state" characterized by a several-fold decrease in input resistance, a depolarized resting potential, and large-amplitude membrane potential fluctuations.⁵⁷ In fact, computational modeling indicates that less than 10% of the input resistance of a cortical neuron is due to voltage-gated channels under these conditions, while synaptic conductances

are 7–30 times larger than somatic leak conductances,⁵⁸ meaning that the majority of membrane conductance at resting potentials is through postsynaptic ion channels.

The effect of background synaptic conductances on photomanipulation of neural activity is illustrated in Figure 8, which depicts the effect of 200 pA photostimulatory (Figure 8C,D) or photoinhibitory (Figure 8E,F) current pulses in a published point conductance model of a neuron in a high-conductance state.⁵⁶ The right column (Figure 8D,F) shows the full model, representing the high-conductance state. In the left column (Figure 8C,E), the variance of background synaptic conductance is decreased 10-fold, simulating conditions *in vitro*, while current is injected through an electrode to depolarize the cell to match firing rates *in vivo*. Photostimulation in the low-conductance state reliably elicits temporally precise spiking (Figure 8C), while the same photostimulation sequence in the high-conductance state increases firing rate slightly (Figure 8D) but is unable to control spiking reliably. Similarly, photoinhibition in the low-conductance state prevents the occurrence of even a single spike (Figure 8E), while identical photoinhibitory currents under realistic high-conductance conditions decrease the spike rate somewhat (Figure 8F) but are unable to prevent firing.

Although neurons *in vivo* are overall less responsive to depolarizing stimuli than neurons *in vitro*, a stochastic resonance phenomenon involving increased membrane potential variability *in vivo* paradoxically enables neurons to respond, albeit with low probability, to stimuli that would always be subthreshold *in vitro*.⁵⁹ Decreases in the membrane time constant associated with the high-conductance state also increase the temporal precision of neuronal responses,⁶⁰ even while the overall response reliability is decreased. Care must therefore be taken in extrapolating from results obtained *in vitro* or under anesthesia to expected performance in awake behaving animals, particularly when the induced photocurrents are small.

3.3. Thermal Photostimulation

The simplest photostimulation method is irradiation of tissue with infrared laser pulses at power levels on the same order as, but less than, the tissue damage threshold. This has been shown to elicit action potentials in exposed peripheral nerve⁶¹ through local heating,⁶² likely via temperature-dependent gating of Na⁺ channels (Figure 9A). Since endogenous large-conductance channels are affected by the temperature shift, action potentials can reliably be induced with high temporal precision. This method may have important applications in clinical neurophysiology, where it is highly advantageous to record physiologic signals directly from human subjects without electrical stimulation artifacts. However, thermal stimulation requires high light intensity and does not provide single-cell spatial resolution or genetic specificity of photostimulation. In experimental animals, these drawbacks could potentially be overcome by expressing heat-sensitive transient receptor potential (TRP) channels in the neurons targeted for stimulation.^{10,63}

3.4. Reactive Oxygen Species-Mediated Photostimulation

Photostimulation with single-cell resolution can be achieved by irradiation at 488 nm⁶⁴ or two-photon irradiation with a pulsed infrared laser,⁶⁵ which enables better depth penetration

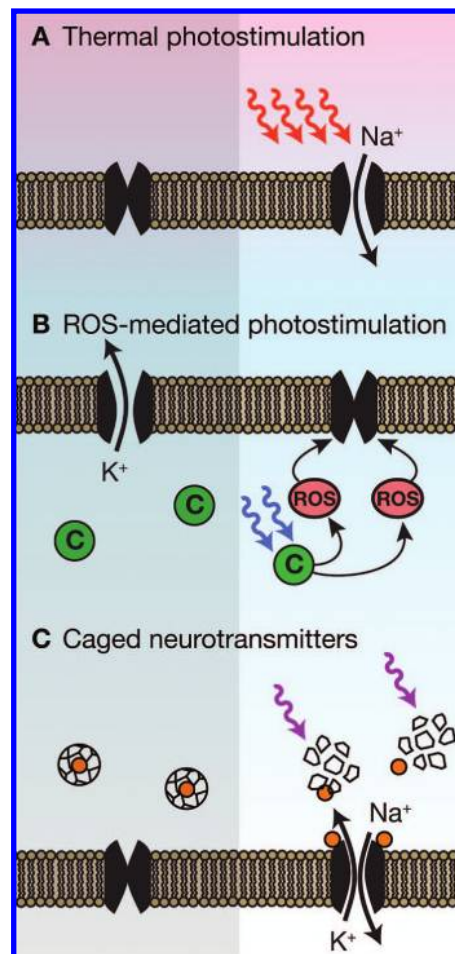


Figure 9. Photomodulation of indirectly light-sensitive conductances: (A) thermal photostimulation with infrared light, likely mediated by temperature-dependent gating of voltage-gated cation channels; (B) photostimulation via ROS generation by intracellular light-absorbing molecules (C); (C) a caged neurotransmitter undergoes photolysis, releasing free agonist. The physiologic effect depends on the type of conductance controlled by the agonist (cf. Figure 7). In the example depicted here, the agonist (e.g., glutamate) opens a nonselective cation conductance, leading to membrane depolarization and action potential firing. Increasing membrane chloride conductance (e.g., via photolysis of caged GABA; not shown) has the opposite effect, activating GABA receptors and decreasing the cell's responsiveness to excitatory synaptic inputs. Caged neurotransmitters are capable of genetic resolution if the photoreleased agonist (the key) lacks endogenous receptors but instead requires the ectopic expression of an "orthogonal" conductance (the lock). Examples of such photochemical "key-and-lock" mechanisms include caged capsaicin gating ectopically expressed TRPV1 and caged ATP gating ectopically expressed P2X₂.

and restriction of the stimulus to a single focal plane. Similar to targeted photoablation, these methods are believed to act primarily through generation of ROS by photoexcitation of endogenous molecules (Figure 9B). The exact mechanism by which ROS generation leads to membrane depolarization most likely involves inhibition of voltage-gated K⁺ channels,⁶⁶ though other mechanisms may also play a role.⁶⁷ As is true in photoablation, addition of exogenous small molecule dyes can sensitize neurons to this method of photostimulation.⁶⁸ Although genetic methods have been used to restrict dye labeling to a subset of cells,^{35,38,39} the use of these technologies for photostimulation has not been reported. As in thermal photostimulation, endogenous high-conductance channels are modulated, enabling reliable control. However, the primary disadvantage of this class of

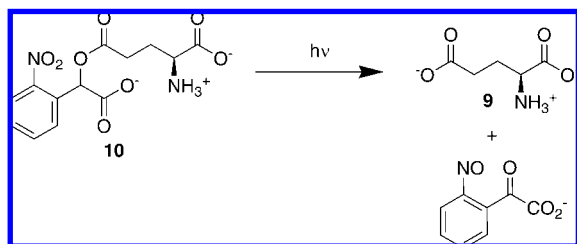


Figure 10. Photolysis of CNB–glutamate.

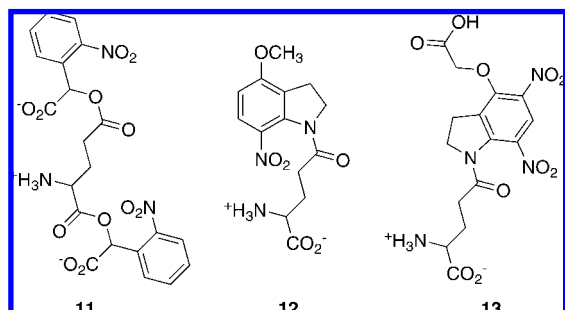


Figure 11. Caged glutamates.

methods is that the ROS generated by the excited chromophore lead rapidly to phototoxicity and cell death, limiting the number of times a cell can be activated.

3.5. Caged Glutamate

The most widespread application of photostimulation has been using “caged glutamate,”^{69,70} which is glutamate, **9** (Figure 10), conjugated with photolabile protecting groups such as the α -carboxy-2-nitrobenzyl (CNB) cage^{71–73} to create CNB–glutamate, **10**. Upon absorption of a single UV photon, the caging group is removed, converting CNB–glutamate to biologically active glutamate, which serves as the most common excitatory neurotransmitter in the CNS of vertebrates. The free glutamate then binds to endogenous ionotropic glutamate receptors, which are ligand-gated nonselective cation channels expressed in the vast majority of CNS neurons; the opening of these conductances depolarizes the membrane (Figure 9C).

Glutamate uncaging has been used for many purposes, most notably to study synaptic plasticity and map receptor densities,^{74–76} as well as to delineate connectivity within cortical circuits.^{69,77–82} One drawback of CNB–glutamate is that photons above and below the focal plane interact with caged molecules, causing uncaging at unintended sites; scattering of UV photons in tissue compounds this problem. To improve resolution in the z -axis, two-photon uncaging was developed,^{83,84} in which two photons are required to uncage the neurotransmitter molecule, largely limiting uncaging to a small (femtoliter) focal volume. In the case of glutamate, this was first accomplished through “chemical two-photon uncaging”, in which two CNB caging groups were conjugated to each glutamate molecule,⁸⁵ **11** (Figure 11), resulting in a significant improvement in axial resolution.⁸⁶ The development of caged molecules with larger two-photon absorption cross sections, such as methoxy-nitroindolino-glutamate^{87,88} (MNI–glutamate, **12**), later enabled optical two-photon uncaging with pulsed infrared lasers. Two-photon uncaging of MNI–glutamate achieves sufficiently fine spatial resolution to restrict activation to individual dendritic spines⁸⁸ and sufficiently deep tissue penetration to map synaptic connectivity in thick brain

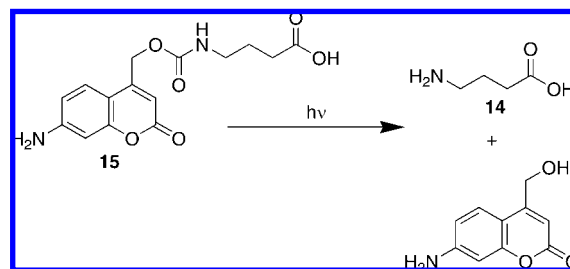


Figure 12. Photolysis of caged GABA (BC204).

slices.⁸⁹ The recent development of glutamate conjugated to the higher efficiency 4-carboxymethoxy-5,7-dinitroindolino (CDNI) caging group,⁹⁰ **13**, which has a quantum yield several times higher than MNI, promises to extend this technology even further by increasing uncaging speed and decreasing residual phototoxicity.⁹¹

Glutamate uncaging has several important advantages, including high speed, precise control of the stimulus in time and in three spatial dimensions, and modulation of endogenous postsynaptic receptors, which mimics physiologic inputs to the cell and enables reliable induction of action potentials. The primary disadvantages of glutamate uncaging are the requirement for expensive exogenous compounds and the fact that glutamate receptors are expressed in almost all cells of the mammalian CNS; both of these severely limit applicability of glutamate uncaging *in vivo*, particularly in deeper cortical layers and other regions for which imaging-quality optical access is not readily available.

3.6. Caged GABA

Analogous to caged glutamate, caged γ -amino-butyric acid (GABA) is an inactive photolabile derivative of GABA, **14** (Figure 12), the primary inhibitory neurotransmitter of the vertebrate CNS. Upon absorption of a photon, caged GABA converts to biologically active GABA, which then binds to and opens ligand-gated chloride channels called GABA_A and GABA_C receptors (Figure 9C); action potential firing is inhibited by hyperpolarizing or shunting inhibition. Other effects on cellular excitability are mediated by GABA_B receptors, which are heterodimeric G protein coupled receptors that lead indirectly to K⁺ channel opening, also inhibiting action potentials.

Early attempts to synthesize caged GABA led to GABA derivatives with unfavorable properties, including GABA receptor antagonist activity^{87,92} and high laser power requirements.⁹³ Recently, a coumarin-based caging group was used to generate 4-[(2*H*-1-benzopyran-2-one-7-amino-4-methoxy)carbonyl]amino]butanoic acid⁹⁴ (BC204, **15**), the first caged GABA with favorable optical and pharmacologic properties comparable to caged glutamate. Since most neurons of the mammalian CNS express GABA receptors, caged GABA allows rapid, precise, generally applicable photoinhibition. Like caged glutamate, however, the cost of the reagents and the lack of genetic resolution are likely to limit applicability *in vivo*. Nevertheless, the combination of caged GABA with caged glutamate finally enables precise photocontrol of both major classes of synaptic input to CNS neurons. Further development of two-photon caging groups with shifted absorption spectra⁹⁵ coupled with advances in fast, three-dimensional beam scanning for femtosecond pulse lasers^{96,97} may one day allow rapid two-photon uncaging of glutamate and GABA with different wavelengths in the same preparation, enabling the artificial creation of arbitrary three-

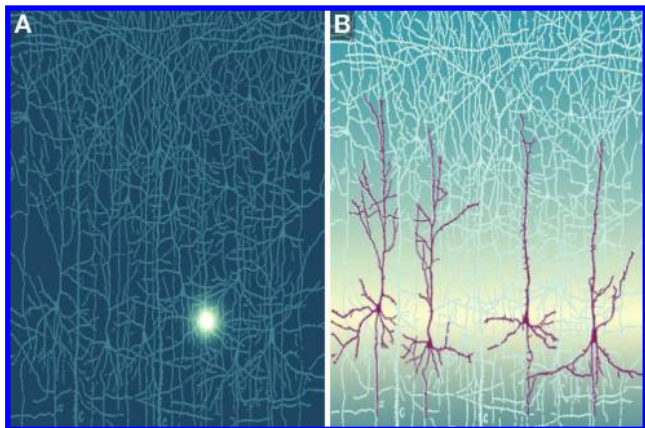


Figure 13. Photomanipulation with and without genetic resolution: (A) in the absence of genetic resolution, the specificity of photomanipulation derives from the precise spatial location of a focused optical stimulus; (B) with genetic resolution, only neurons expressing a directly or indirectly light-sensitive protein are responsive to the optical stimulus, which can now be focused or broad.

dimensional patterns of excitatory and inhibitory synaptic input simultaneously, in real time, with single-synapse spatial resolution.

3.7. Genetically Encoded Photomodulators of Membrane Potential

The second broad class of photostimulation technologies utilizes genetically encoded, light-controlled actuators to restrict photosensitivity by gene expression rather than spatial location alone.^{4,8} The primary advantage of these methods is their “genetic resolution”: the ability to target subsets of cells within an anatomic structure or region based on cell type or connectivity (Figure 13). As a result, these approaches are most advantageous when specific cell types need to be controlled in situations where imaging-quality optical access is not available. For experiments in which entire anatomic structures or regions are to be targeted, electrode-based microstimulation, lesioning, and drug infusion techniques are likely to be superior.

Almost all genetically encoded photomanipulation technologies share a fundamental mechanism: light sensitivity is provided by a small molecule that undergoes a chemical change upon illumination, leading directly or indirectly to modulation of ion channels in the membrane. Based on the identity of the light-sensitive molecule, these technologies can be categorized into two broad groups: those based on retinal,^{8,12,13,15,16} an endogenous vitamin A derivative, and those based on exogenous light-sensitive small molecules.^{10,11,14}

3.7.1. Rhodopsins

Retinal is the basis of light sensitivity in two large classes of light-sensitive proteins known as opsins in pure protein form or as rhodopsins when in complex with retinal. The first class is G protein coupled opsins, while the second is microbial opsins. Both classes have seven α -helical trans-membrane domains and a deep retinal binding pocket that is accessed from the extracellular side. In both classes of opsins, the retinal chromophore forms a covalent Schiff base linkage to a conserved lysine residue in the protein; however, low sequence homology between the two classes suggests that they are in fact unrelated,⁹⁸ representing instead an interesting case of convergent evolution.

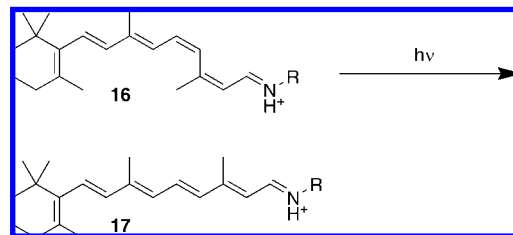


Figure 14. 11-*cis*-Retinal and all-*trans*-retinal.

The first class, G protein coupled rhodopsins, are prototypical G protein coupled receptors that are activated by light. The chromophore of these rhodopsins is 11-*cis*-retinal, **16**, or a hydroxylated derivative. The 11-*cis* isomer **16** is converted to all-*trans*-retinal, **17**, by absorption of a photon (Figure 14). Isomerization of the chromophore switches the rhodopsin molecule to an active metarhodopsin form, which catalyzes nucleotide exchange on its cognate heterotrimeric G protein, thereby initiating an intracellular signaling cascade (Figure 15A,B).

The best-characterized rhodopsins are found in vertebrate and invertebrate visual systems and differ in two important ways. First, vertebrate visual rhodopsins in photoreceptor cells signal through G_t , or transducin, leading to activation of cyclic GMP phosphodiesterase. Light activation of these rhodopsins thus causes a drop in the concentration of cyclic GMP, which closes cyclic GMP-gated Na^+ channels and hyperpolarizes the cell. Invertebrate visual rhodopsins, in contrast, signal through G_q , which leads through a poorly understood mechanism to activation of nonselective cation channels and cell depolarization. Second, vertebrate visual opsins catalyze hydrolysis of the Schiff base linkage after photon absorption and rapidly dissociate from the all-*trans*-retinal chromophore, thus requiring a constant supply of 11-*cis*-retinal to replenish the bleached all-*trans* isomer.⁹⁹ Invertebrate visual opsins instead remain bound to the all-*trans*-retinal after initial photoisomerization and depend on the absorption of a second photon at a shifted wavelength to convert the all-*trans* back to the 11-*cis* isomer. In other words, invertebrate visual opsins possess intrinsic photoisomerase activity, unlike vertebrate visual opsins, which require an additional biochemical pathway not present in most neurons.

3.7.1.1. ChARGe. The first application of rhodopsins to photostimulation was the chARGe system (Figure 15A), in which neurons were rendered light responsive by the expression of three proteins from the *Drosophila* visual phototransduction cascade.⁸ The name chARGe refers to these proteins: arrestin, rhodopsin, and $G\alpha$. Since chARGe uses a *Drosophila* visual rhodopsin, signaling occurs through the $G_{q/11}$ class of G proteins, the α subunit of which comprises the second component of the system, leading to opening of endogenous nonselective cation channels in the plasma membrane (Figure 5A). Binding of arrestin, the third component of the system, then inactivates the metarhodopsin state and initiates the biochemical cycle that regenerates 11-*cis*-retinal.

In addition to being the prototype of all genetically targeted photomodulation approaches, chARGe possesses several practical advantages. The signal resulting from the activation of a rhodopsin molecule is biochemically amplified so that the absorption of a single photon can modulate many endogenous conductances; this cascade underlies the high light sensitivity of photoreceptor cells. Additionally, the

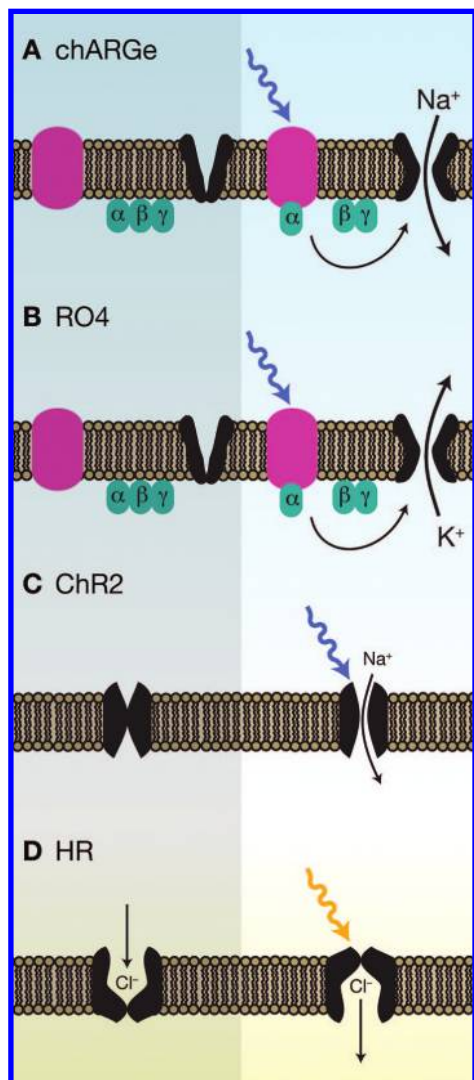


Figure 15. Photomanipulation of ionic currents via rhodopsins: (A) In the chARGe system, photoisomerization of bound 11-*cis*-retinal to all-*trans*-retinal initiates signaling through the $G_{q/11}$ pathway, leading to the opening of nonselective cation conductances. (B) With RO4, photoisomerization of bound 11-*cis*-retinal to all-*trans*-retinal initiates signaling through the $G_{i/o}$ pathway, leading to opening of GIRK potassium channels. (C) Photoisomerization of channelrhodopsin-2 (ChR2)-bound all-*trans*-retinal to 13-*cis*-retinal initiates a photocycle, in which the channel protein passes through multiple open states, allowing nonselective passage of cations. (D) Photoisomerization of halorhodopsin (HR)-bound all-*trans*-retinal to 13-*cis*-retinal initiates a photocycle, resulting in the translocation of a single chloride ion from the extracellular to the intracellular space.

photocycle of *Drosophila* visual rhodopsin continuously regenerates 11-*cis*-retinal. Although chARGe has never been tested in mammalian cells *in vivo*, the decreased retinal requirement relative to vertebrate visual rhodopsins would likely be satisfied by endogenous stores, obviating the need for addition of exogenous retinal.

The primary disadvantages of chARGe include relatively slow on–off kinetics on the order of seconds,⁸ as well as the fact that three separate genes must be introduced, complicating genetic schemes. It is worth noting that melanopsins, a class of mammalian opsins closely related to invertebrate rhodopsins, have been shown *in vitro* to depolarize mammalian cells (but not *Xenopus* oocytes¹⁰⁰) without introduction of exogenous $G\alpha$ or arrestin.^{101,102} This observation suggests that, at least in some neurons, only the

opsin gene may be necessary. Since chARGe modulates endogenous cation channels, however, the introduction of additional channel genes may be necessary if expression levels of those channels are insufficient in a given neuron population. This would not only further complicate genetic schemes but also run the risk of perturbing normal neuronal physiology.

3.7.1.2. RO4. Vertebrate visual rhodopsins, such as rat rhodopsin 4 (RO4), have also been used for photomodulation of neural activity¹³ (Figure 15B). In retinal photoreceptor cells, which are not considered neurons in vertebrates, rhodopsins signal through the G protein transducin, the α -subunit of which belongs to the same family as the pertussis toxin-sensitive $G_{i/o}$ subtypes. Since transducin is not present in most neurons, RO4 signals instead through the endogenous $G_{i/o}$ pathway and thus inhibits action potentials by increasing the cell's K^+ conductance through G protein-activated inwardly rectifying K^+ (GIRK) channels. Interestingly, RO4 signaling is also capable of modulating presynaptic Ca^{2+} channels,¹³ decreasing vesicle release probability and corresponding excitatory postsynaptic current (EPSC) amplitude by 40%. Like chARGe, RO4 displays relatively slow on/off kinetics and is dependent on the modulation of endogenous channels, meaning that overexpression of GIRKs may be required if cellular expression is insufficient. In RO4-expressing cultured hippocampal neurons, which are in a low-conductance state, illumination reduced the number of action potentials evoked by current injection by over 50% but was not capable of eliminating firing entirely.¹³ Although results in chick embryonic spinal cord in isolation and *in ovo* are encouraging,¹³ it remains to be seen whether the small conductances induced by RO4 will have a significant effect under the high-conductance conditions encountered in mammalian neurons *in vivo*.

A second barrier to utilization of RO4 in the CNS is the photocycle of mammalian visual rhodopsins, in which the bleached all-*trans*-retinal isomer is expelled from the opsin and isomerized by a specialized biochemical pathway.⁹⁹ While similar retinoid processing pathways are found in unexpected places, such as HEK293S cells,¹⁰³ it is unknown whether such pathways are functional in the intact mammalian brain. As a result, successful use of RO4 under conditions of limited retinal supply—in intact mammals, for example, but perhaps not in chick embryos¹³—may require either loading with 9-*cis*-retinal,¹⁰⁴ a commercially available analog of the 11-*cis* retinal chromophore, or the introduction of additional genes reconstituting the isomerization pathway.

3.7.1.3. Channelrhodopsin-2. The second class of rhodopsins, microbial rhodopsins, is best known for its most thoroughly characterized member, bacteriorhodopsin, a photosynthetic ion pump. Reflecting their lack of sequence homology, microbial rhodopsins differ from G protein coupled rhodopsins in three important ways. First, rather than signaling through G protein mediated cascades, most microbial rhodopsins are ion pumps that move protons or chloride ions unidirectionally across the membrane. Second, the chromophore of microbial opsins is all-*trans*-retinal (**17**), which is converted by the absorption of a photon to 13-*cis*-retinal, **18** (Figure 16), initiating a photocycle; in G protein-coupled rhodopsins, in contrast, an 11-*cis*-retinal chromophore **16** converts to all-*trans*-retinal **17** upon illumination (Figure 14). Finally, microbial rhodopsins retain the bleached retinal isomer and independently catalyze isomerization back to the unbleached form. This self-contained photocycle is

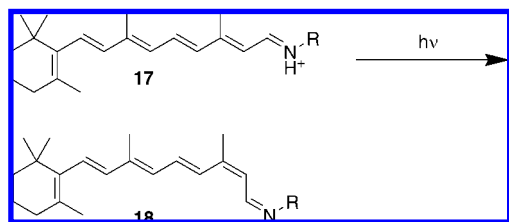


Figure 16. All-*trans*-retinal and 13-*cis*-retinal

reminiscent of melanopsins or invertebrate visual rhodopsins but distinct from vertebrate visual rhodopsins. Since a constant supply of unbleached retinal is not required, endogenous retinal levels in the mammalian CNS are sufficient to form functional microbial rhodopsins, at least in the case of channelrhodopsin-2.

Channelrhodopsin-2 (ChR2), a eukaryotic homologue of bacteriorhodopsin,^{105–107} is an unusual member of a family composed mostly of light-driven ion pumps: it is a nonselective cation channel gated directly by light.¹⁰⁶ Like bacteriorhodopsin, ChR2 undergoes a photocycle upon absorption of a photon, which involves transitioning through several kinetic intermediates. Unlike bacteriorhodopsin, however, ChR2 possesses two or more intermediates in which the molecule acts as a nonselective cation channel¹⁰⁸ with a reversal potential near 0 mV (Figure 15C).

The primary advantage of ChR2 is its simplicity: only one gene must be introduced, the retinal cofactor is present at sufficiently high concentrations *in vivo*, and the protein lacks known homologues in multicellular organisms, making it unlikely to interfere with normal cellular processes. ChR2 also has rapid kinetics, with $\tau_{\text{on}} < 200 \mu\text{s}$ and $\tau_{\text{off}} \approx 20 \text{ ms}$,¹⁰⁶ enabling temporally precise control of photostimulation.^{12,13} Another important feature of ChR2 is that the energy barrier to initiation of a photocycle is large, and thermal isomerizations are rare, meaning that the leak conductance in the absence of illumination is virtually zero; consistent with this, neurons expressing ChR2 possess normal electrophysiological excitability and resting membrane potential.^{12,13,19}

The flip side of this feature represents the primary drawback of ChR2, which is its low unitary conductance estimated at $\sim 50 \text{ fS}$.¹⁰⁶ To put this in perspective, the single-channel conductance of ChR2 is ~ 400 -fold lower than the unitary conductance of the prototypical Shaker K^+ channel.¹⁰⁹ As a result, high expression levels and illumination intensities are required to drive neurons to firing threshold. In one study,¹² for example, ChR2 was expressed in cultured neurons using a strong promoter and lentiviral transfection, enabling extremely high expression levels. Despite otherwise favorable conditions of excellent optical access and neurons in a low-conductance state, optical stimulation induced reliable spiking in only 13 of 18 neurons tested.¹²

The problem of low ChR2 conductance was partially rectified through the use of the H134R mutation, which increases peak currents by ~ 2.4 -fold and steady-state currents by ~ 1.7 -fold.^{110,111} However, high expression levels are still required, favoring the use of viral expression or electroporation *in utero* over genomic integration. Nevertheless, ChR2 has been used successfully in transgenic mice when expressed from a strong promoter^{17,19} and, as is the rule in this setting, high transgene copy numbers. The use of codon-optimized ChR2 also boosts expression levels,¹⁵ which, however, must be titrated carefully to avoid toxicity.¹¹¹

ChR2 has proven a powerful and versatile tool for such diverse applications as mapping synaptic connectivity,^{17–19}

correlating physiologic responses with anatomic projection patterns,²⁷ probing the role of hypocretin neurons in sleep/wake transitions,²² studying the role of dopaminergic and octopaminergic systems for learning in *Drosophila* larvae,²¹ defining the sensory signals carried by specific classes of peripheral neurons in adult flies,²³ estimating the number of cortical action potentials necessary for perceptual decisions,²⁶ and even treating blindness in mice with photoreceptor degeneration.¹¹²

It is worth noting that all published reports to date containing physiological recordings of ChR2-expressing cells *in vivo* were performed in anesthetized animals, in which neurons are in low-conductance states characterized by high input resistance and low membrane potential variability. Care must be taken in extrapolating from the reliability of stimulation *in vitro* or in the low-conductance state of anesthesia to the high-conductance and high membrane potential variability states found in behaving animals; the reliability of optical control is likely to be reduced significantly under these conditions (Figure 8C,D).

3.7.1.4. Halorhodopsin. Halorhodopsin (HR) is a well-studied microbial opsin from halophilic archaea that pumps Cl^- ions into a cell against their electrochemical gradient (Figure 15D). Unlike ion channels that introduce conductances, ion pumps inject current directly; the net balance of charges moved across the membrane is therefore only weakly dependent on the membrane potential over physiological ranges. In other words, opening channels tends to bring the membrane potential toward the reversal potential associated with that channel, while activating pumps simply moves the membrane potential in one direction. HR pumps Cl^- ions inward, hyperpolarizing the membrane; in cultured hippocampal neurons, this leads to inhibition of firing, or even the precise deletion of single spikes at their anticipated times in a rhythmic spike train.^{15,16} HR possesses many of the advantages of ChR2, including rapid kinetics, the lack of exogenous cofactors, the simplicity of introducing a single gene, the low likelihood of interacting with endogenous membrane proteins, and the extremely low probability of thermal isomerization.

Like ChR2, however, HR is capable of injecting only small currents. For HR, this problem is even further compounded by the fact that the protein is a pump, not a channel. In ChR2, each photocycle involves at least two conducting intermediates in which many ions flow through the channel; in HR, each photocycle results in the translocation of only one ion. As a result, currents are small, with peak amplitudes ranging from ~ 45 to $\sim 90 \text{ pA}$ ¹⁵ in cultured rat hippocampal neurons expressing codon-optimized HR. In contrast, current amplitudes with ChR2 under similar conditions are $\sim 500 \text{ pA}$ at peak and $\sim 200 \text{ pA}$ at plateau,¹² without codon optimization¹⁵ or the conductance-enhancing H134R mutation.¹¹⁰

It is instructive to place the photocurrents produced by ChR2 and HR on a physiological scale. The average threshold excitatory postsynaptic current (EPSC) required to fire an action potential in a rat hippocampal neuron under low-conductance conditions *in vitro* is $\sim 200 \text{ pA}$,¹¹³ while the average miniature EPSC (i.e., the postsynaptic current produced by presynaptic release of a single glutamate-filled vesicle) is $\sim 8 \text{ pA}$.¹¹³ At high expression levels, ChR2 thus exerts a peak effect on a hippocampal pyramidal cell of roughly the same magnitude as the synchronous presynaptic release of ~ 60 vesicles of excitatory neurotransmitter onto its thousands of input synapses. The peak currents generated

by HR (45–90 pA^{15,16}) under similarly favorable conditions offset the impact of just 5–11 such vesicle release events.

Since cells *in vivo* have many more active synapses than cells *in vitro*, the effect of negating a small number of excitatory synaptic inputs is modest in the intact brain. This is illustrated in Figure 8E,F, which depicts the effects of light-induced 200 pA hyperpolarizing current pulses on firing patterns in a point conductance model of a neuron.⁵⁶ When the variance of synaptic conductance is decreased to 10% of the normal value, simulating the low-conductance state (Figure 8A), light pulses reliably inhibit spiking induced by current injection through the patch electrode (Figure 8E), as is indeed seen *in vitro*.^{15,16} With full synaptic variance, representing the high-conductance state *in vivo*, the same light pulses reduce overall firing rate somewhat but are incapable of inhibiting spiking induced by synaptic inputs (Figure 8F), despite the fact that the mean firing rate in the dark is the same in the low- and high-conductance conditions. Although HR is unlikely to exert the same precise control *in vivo* that can be observed *in vitro*, certain favorable systems may exist where biasing the membrane potential in groups of neurons will lead to behavioral or physiological phenotypes.

3.7.2. Proteins Regulated via Exogenous Light-Sensitive Molecules

The other broad class of genetically encoded photostimulation technologies includes those that combine the expression of exogenous channels with the introduction of light-sensitive small molecule ligands orthogonal to endogenous receptors. The first of these were the combinations of TRPV1 channels with caged capsaicin¹⁰ and ATP-gated P2X receptors with caged ATP.¹⁰ Later variations include SPARK¹¹ and LiGluR,¹⁴ which are based on the selective covalent attachment of light-sensitive affinity reagents¹¹⁴ to mutant channels.

3.7.2.1. TRPV1 and Caged Capsaicin. Transient receptor potential (TRP) channels are not typical ligand-gated receptors but rather voltage-gated cation channels highly homologous to the prototypical Shaker K⁺ channel but without potassium selectivity. The voltage-dependent gating curves of some TRP channels are shifted by changes in temperature or binding of molecules such as capsaicin (TRPV1) and menthol (TRPM8), causing these channels to behave as temperature- and ligand-gated receptors.^{63,115–117} Temperature sensation is an important physiologic role of TRP channels in humans, explaining the subjective “hot” sensation evoked when capsaicin in chili peppers activates TRPV1-expressing sensory neurons in the tongue.¹¹⁵ Since TRPV1 expression is largely confined to the peripheral nervous system,¹¹⁵ TRPV1 can be heterologously expressed in CNS neurons, where addition of capsaicin causes opening of TRPV1 channels, depolarizing the membrane and inducing action potential firing.¹⁰ In addition, capsaicin (**19**) and related vanilloids can be conjugated with photolabile protecting groups to form biologically inert compounds (Figures 17 and 18), such as 4,5-dimethoxy-nitrobenzyl (DMNB)–capsaicin (**20**),¹⁰ *N*-(2-nitrobenzyl)-*N*-vanillyl-nonanoylamide (Nb-VNA, **21**),¹¹⁸ *N*-(4,5-dimethoxy-2-nitrobenzyl)-*N*-vanillyl-nonanoylamide (Nv-VNA, **22**),¹¹⁸ α -carboxy-4,5-dimethoxy-2-nitrobenzyl (CDMNB)–capsaicin (**23**),¹¹⁹ and {7-[bis(carboxymethyl)amino]coumarin-4-yl}methoxycarbonyl (BCMCMOC)–capsaicin (**24**).¹¹⁹ All of these compounds convert to active TRPV1 agonists upon illumination

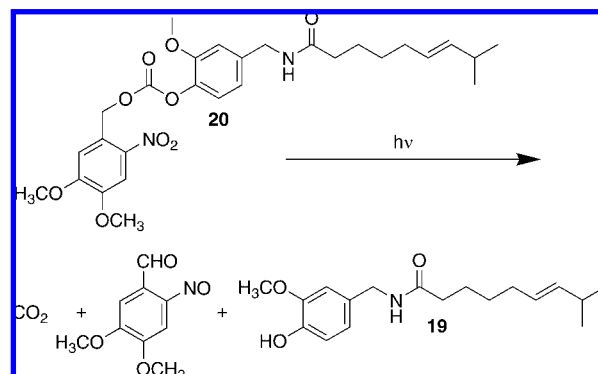


Figure 17. Photolysis of DMNB–capsaicin.

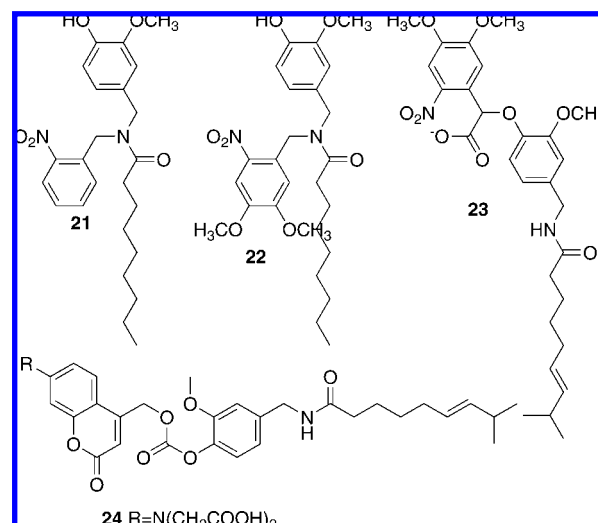


Figure 18. Caged vanilloids.

(Figure 9C) and can be used to induce action potential firing in TRPV1-expressing neurons *in vitro* with light.^{10,119}

The primary advantage of TRPV1 is the large unitary conductance of ~ 35 pS,¹¹⁵ which permits effective photomodulation of membrane potential even at low channel densities. In fact, application of low capsaicin concentrations to cultured rat hippocampal neurons expressing TRPV1 leads to reliable action potential firing,¹⁰ while high capsaicin concentrations overpower endogenous voltage-gated conductances, leading to the membrane potential being clamped near the TRPV1 reversal potential.¹⁰ A second advantage is the capacity to employ nonlinear optics, that is, multiphoton uncaging,^{83,84} to localize the release of capsaicin precisely in three spatial dimensions;¹¹⁸ multiphoton excitation of G protein coupled and microbial rhodopsins, in contrast, has not been reported.

The principal disadvantages include kinetics on a time scale of tens to hundreds of milliseconds,¹⁰ TRPV1-mediated leak currents potentially interfering with normal cell physiology, the possibility of heterotetramerization with endogenous TRP channel subunits, and the fact that endogenous TRPV1 expression in some regions of the mammalian CNS has been reported,¹²⁰ which could potentially lead to undesirable cross-talk. The requirement for loading of caged ligand limits optical applications in the intact vertebrate brain, but the ability to control genetically targeted neurons pharmacologically¹²¹ may be a very significant plus when manipulation of activity at rapid time scales is not essential.

3.7.2.2. P2X₂ and Caged ATP. P2X₂ is an ATP-gated nonselective cation channel possessing one of the simplest

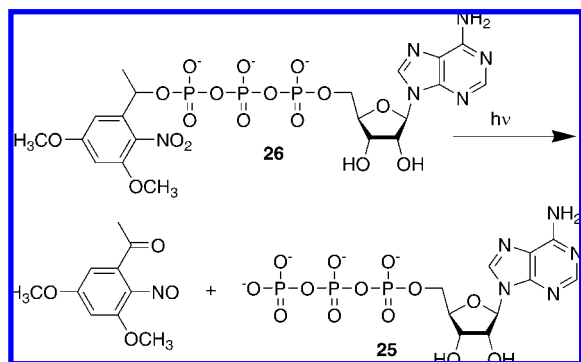


Figure 19. Photolysis of DMNPE–ATP.

architectures of known ligand-gated channels: it is a homotrimer where each subunit comprises two transmembrane domains and a large extracellular ligand-binding domain.^{122,123} Adding ATP to cultured hippocampal neurons expressing a covalently linked trimer of P2X₂ subunits has been shown to lead reliably to P2X₂ channel opening, membrane depolarization, and firing of action potentials.¹⁰ Since ATP, **25** (Figure 19), can be conjugated to photolabile cages, such as the *P*³–[1-(4,5-dimethoxy-2-nitrophenyl)ethyl] (DMNPE) protecting group,^{124,125} **26**, light pulses can also be used to evoke reliable trains of action potentials in P2X₂-expressing neurons¹⁰ (Figure 9C).

The advantages and disadvantages of P2X₂ parallel those of TRPV1: a large unitary conductance of ~30 pS,¹²⁶ kinetics on a time scale of tens to hundreds of milliseconds,^{10,20} the ability to restrict two-photon activation to the focus of an uncaging beam but also the need to deliver potentially copious quantities of exogenous compounds, and, for mammals, possible cross-talk via endogenous ATP receptors. Additionally, leak currents in the absence of ATP have been shown to alter the behavior and shorten the lifespan of flies that massively overexpress P2X₂.²⁰ It is unclear to what extent these leak currents are mediated by the low, but potentially significant, channel open probability in the absence of ATP, as opposed to the activation of receptors by the co-release of ATP from synaptic vesicles¹²⁷ during transmission.

P2X₂ receptor-mediated photostimulation in *Drosophila*, an organism without endogenous ATP-gated channels, has led to novel insights into the role of dopaminergic circuits in the organization of exploratory movements²⁰ and into some of the neural mechanisms underlying sexually dimorphic behavior.²⁵ Stimulating a circuit of ~200 neurons controlling the production of the male-specific courtship song revealed that a song-like motor program is present also in females but normally activated only in males. The circuit's internal dynamics also differed between sexes: although the artificially evoked female songs replicated some of the typical acoustic structure of males, the sonic output of females was too far off key to produce effective mating signals.²⁵

3.7.2.3. SPARK. The synthetic photoisomerizable azobenzene-regulated K⁺ channel, or SPARK,¹¹ uses the combination of mutant K⁺ channels and light-sensitive small molecules to inhibit neuronal firing with light. The channel component consists of a Shaker K⁺ channel mutated to remove fast N-type inactivation, reduce slow C-type inactivation, and shift gating to hyperpolarized potentials. These modifications result in a K⁺ channel that possesses a significant open probability at resting membrane potentials, thus hyperpolarizing the membrane and inhibiting firing. The

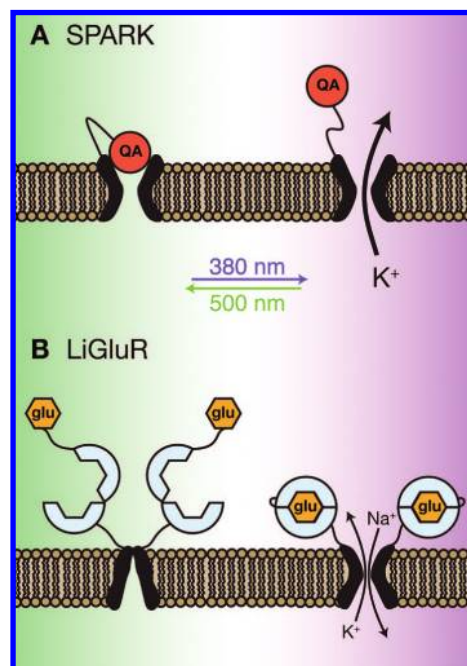


Figure 20. Engineered photoswitchable conductances: (A) SPARK. In darkness, the MAL-AZO-QA molecule slowly relaxes to the longer *trans* conformation, allowing the quaternary ammonium group (QA, red) to block a constitutively open K⁺ channel. When transiently illuminated with 380 nm light, the MAL-AZO-QA molecule rapidly converts to the *cis* isomer, unblocking the K⁺ channel and hyperpolarizing the cell. The MAL-AZO-QA molecule will remain in the *cis* state for many minutes but can be rapidly converted to the channel-blocking *trans* state by transient illumination at 500 nm. (B) LiGluR. In darkness, the MAG molecule slowly relaxes to the *trans* conformation, preventing the glutamate analog (glu, yellow) from reaching its binding site on an engineered variant of the iGluR6 glutamate receptor. When transiently illuminated with 380 nm light, the MAG molecule rapidly converts to the *cis* isomer, allowing the glutamate analog to bind to the receptor, open a nonselective cation conductance, and depolarize the cell. The MAG molecule will remain in the *cis* state for many minutes but can be rapidly converted to the *trans* conformation by transient illumination at 500 nm.

channels also contain an additional mutation that introduces an extracellular cysteine near the binding site for tetraethylammonium (TEA), a K⁺ channel blocker. The small molecule MAL-AZO-QA is then added, which is composed of a maleimide group to anchor the molecule to the introduced cysteine, a photoisomerizable azobenzene linker, and a quaternary ammonium (QA) group that binds to the TEA site, blocking the channel pore (Figure 20A). In the dark state, the rigid azobenzene linker remains in the lower-energy *trans* configuration, **27** (Figure 21), which has a length of ~17 Å, long enough for the QA group to reach the TEA binding site and block the K⁺ channel. Brief pulses of light at 380 nm isomerize the AZO linker to the high-energy *cis* configuration **28** and unblock the channel pore, thereby hyperpolarizing the membrane and inhibiting firing. Another brief light pulse at 500 nm converts the linker back to the *trans* isomer and reblocks the pore. The active *cis* state is stable for several minutes in the dark, enabling prolonged photoinhibition by a single pulse at 380 nm.

The main advantages of this method include submillisecond on/off kinetics and the large unitary conductance of ~20 pS,¹⁰⁹ which should enable reliable inhibition of action potentials even at relatively low expression levels. Also, neurons can be stably inhibited in the dark for many minutes following a single light pulse.

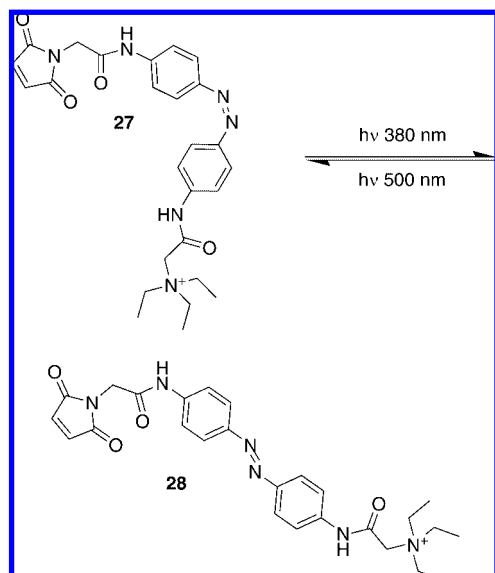


Figure 21. Photoisomerization of MAL-AZO-QA.

Despite the elegance of this approach, SPARK suffers from a number of practical disadvantages. First, Shaker channels are tetramers, and the SPARK channel would heterotetramerize with endogenous channel subunits,¹²⁸ altering channel properties. Subunit mixing may be particularly problematic *in vivo*, as endogenous K^+ channels are expressed at lower levels than what is typically required to visualize GFP, for example, and these K^+ conductances may be perturbed by weak promoter leakage even in “negative” cells where a fluorescent marker protein is not visible. Future versions of SPARK may rectify this problem by using different K^+ channels or by covalently linking four subunits of Shaker channels¹²⁸ with the T1 tetramerization domain removed.¹²⁹

An additional problem is that SPARK channels have an increased open probability at resting potentials, which leads to chronic hyperpolarization of the membrane in the developmental period prior to the introduction of MAL-AZO-QA. Overexpression of K^+ channels has been shown to cause compensatory up-regulation of other ion channels,¹³⁰ leading to hyperexcitability; in some cases, however, increased K^+ channel expression has also been found to lead directly to cell death.¹³¹ These problems could potentially be mitigated by inducing the expression of SPARK immediately before or during the application of MAL-AZO-QA. Finally, the use of ultraviolet wavelengths and the need to deliver MAL-AZO-QA complicate use in deep structures of larger animals.

3.7.3.4. LiGluR. Light-gated ionotropic glutamate receptor, or LiGluR,¹⁴ combines a mutant glutamate-gated non-selective cation channel with a light-sensitive small molecule affinity ligand¹¹⁴ covalently attached to the channel (Figure 20B). Analogous to SPARK, site-specific labeling is accomplished by mutating ionotropic glutamate receptor 6 (iGluR6) to introduce an extracellular cysteine residue a measured distance away from the ligand binding pocket, followed by adding a small molecule known as MAG: maleimide anchor–azobenzene linker–glutamate analog (Figure 22). The maleimide anchors the molecule to the introduced cysteine, while the *trans*-azobenzene linker holds the terminal glutamate analog near to, but not in contact with, the glutamate binding site of the channel. A short pulse of light at 380 nm isomerizes the *trans*-azobenzene linker, **29**, to the higher-energy *cis* form, **30**, enabling the glutamate

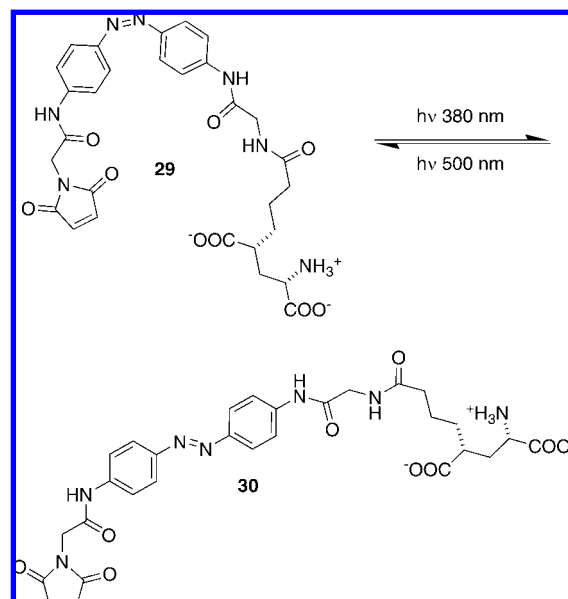


Figure 22. Photoisomerization of MAG.

analog to access the binding site and open the channel. In darkness, the *cis*-azobenzene slowly decays to the lower-energy *trans* form with a half-life of ~ 18 min, meaning that neurons can be stably depolarized for many minutes in response to a single pulse of light. However, the *cis*-azobenzene can also be rapidly isomerized back to the inactive *trans* form with a brief pulse of light at 500 nm. Pulses of light at intermediate wavelengths between 380 and 500 nm fix a certain proportion of LiGluR molecules in the active state, enabling analog regulation of photostimulation intensity.²⁴

The advantages of this method include the extremely fast on/off kinetics, the fact that prolonged excitation can be achieved by a single pulse of light, and the large unitary conductance of the channel relative to ChR2. At ~ 250 fS,¹³² the unitary conductance of GluR6 homotetramers is still quite small but approximately 5-fold larger than that of ChR2;¹⁰⁶ correspondingly, LiGluR was found to be capable of inducing currents approximately 5-fold larger than those induced by ChR2 in cultured rat hippocampal neurons under similar conditions.²⁴ There are also disadvantages, such as the likely heteromultimerization of mutant iGluR6 subunits with wild-type iGluR6 subunits, as well as the fact that the mutant iGluR6 subunits still respond to endogenous glutamate release, which may lead to altered physiological signaling. Also, the use of UV light and exogenous ligands complicate stimulation of deeper structures in the intact brains of larger organisms. However, LiGluR was used to disrupt fast escape responses in transgenic zebrafish larvae after incubation in a solution containing MAG and DMSO,²⁴ demonstrating robust performance in at least one behaviorally rich and genetically tractable model system *in vivo*.

4. Conclusion

The nervous system exhibits the most complex anatomical structures and functional dynamics of any organ system. So far, only optical technologies have been able to provide the parallelism, micrometer spatial resolution, and millisecond temporal resolution necessary to manipulate neural activity with a high degree of precision. While many challenges

remain, photoablation and neurotransmitter uncaging, in particular, have already built up solid records of achievement in research.

More recently, light-controlled actuators that can be encoded in DNA have turned the large number of genetically distinct cell types in the brain into natural platforms for exploration. The strategy of encoding sensitivity to light genetically has opened many new possibilities and inspired a ballooning secondary literature, with review articles at this point nearly outnumbering publications of original research—a point we make at no small risk of hypocrisy. Yet our intent here is to stress the importance of tempering enthusiasm for these technologies with realistic expectations. Claude Shannon, the father of information theory, expressed a similar sentiment in a note entitled “The Bandwagon”,¹³³ from which we borrow our conclusion, paraphrasing slightly:

“Although this wave of popularity is certainly pleasant and exciting for those of us working in the field, it carries at the same time an element of danger. While we feel that [genetically encoded optical actuators are] indeed a valuable tool in providing fundamental insights into the function of [neural circuits] and will continue to grow in importance, they are certainly no panacea for the [neuroscientist] or, *a fortiori*, for anyone else. Seldom do more than a few of nature’s secrets give way at one time. It will be all too easy for our somewhat artificial prosperity to collapse overnight when it is realized that the use of a few [light-sensitive molecules] does not solve all our problems.

“What can be done to inject a note of moderation in this situation? In the first place, ... [a] thorough understanding of the [biophysical] foundation ... is surely a prerequisite to other applications. ... Secondly, we must keep our own house in first class order. The subject of [genetically targeted photocontrol of neural activity] has certainly been sold, if not oversold. We should now turn our attention to the business of research and development at the highest scientific plane we can maintain. Research rather than exposition is keynote, and our critical thresholds should be raised.”

5. Acknowledgments

We thank Graham Ellis-Davies and Adam Claridge-Chang for comments. Work in the authors’ laboratory is supported by the NIH, the Charles E. Dana Foundation, the Office of Naval Research, the Medical Research Council (UK), and the Human Frontiers Science Program.

6. References

- Cohen, L. B.; Salzberg, B. M.; Grinvald, A. *Annu. Rev. Neurosci.* **1978**, *1*, 171–182.
- Tsien, R. Y. *Annu. Rev. Neurosci.* **1989**, *12*, 227–253.
- Miesenböck, G. *Curr. Opin. Neurobiol.* **2004**, *14*, 395–402.
- Miesenböck, G.; Kevrekidis, I. G. *Annu. Rev. Neurosci.* **2005**, *28*, 533–563.
- Yuste, R.; Katz, L. C. *Neuron* **1991**, *6*, 333–344.
- Ng, M.; Roorda, R. D.; Lima, S. Q.; Zemelman, B. V.; Morcillo, P.; Miesenböck, G. *Neuron* **2002**, *36*, 463–474.
- Ohki, K.; Chung, S.; Ch’ng, Y. H.; Kara, P.; Reid, R. C. *Nature* **2005**, *433*, 597–603.
- Zemelman, B. V.; Lee, G. A.; Ng, M.; Miesenböck, G. *Neuron* **2002**, *33*, 15–22.
- Crick, F. *Philos. Trans. R. Soc. London, Ser. B* **1999**, *354*, 2021–2025.
- Zemelman, B. V.; Nesnas, N.; Lee, G. A.; Miesenböck, G. *Proc. Natl. Acad. Sci. U.S.A.* **2003**, *100*, 1352–1357.
- Banghart, M.; Borges, K.; Isacoff, E.; Trauner, D.; Kramer, R. H. *Nat. Neurosci.* **2004**, *7*, 1381–1386.
- Boyden, E. S.; Zhang, F.; Bamberg, E.; Nagel, G.; Deisseroth, K. *Nat. Neurosci.* **2005**, *8*, 1263–1268.
- Li, X.; Gutierrez, D. V.; Hanson, M. G.; Han, J.; Mark, M. D.; Chiel, H.; Hegemann, P.; Landmesser, L. T.; Herlitze, S. *Proc. Natl. Acad. Sci. U.S.A.* **2005**, *102*, 17816–17821.
- Volgraf, M.; Gorostiza, P.; Numano, R.; Kramer, R. H.; Isacoff, E. Y.; Trauner, D. *Nat. Chem. Biol.* **2006**, *2*, 47–52.
- Han, X.; Boyden, E. S. *PLoS ONE* **2007**, *2*, e299.
- Zhang, F.; Wang, L. P.; Brauner, M.; Liewald, J. F.; Kay, K.; Watzke, N.; Wood, P. G.; Bamberg, E.; Nagel, G.; Gottschalk, A.; Deisseroth, K. *Nature* **2007**, *446*, 633–639.
- Arenkiel, B. R.; Peca, J.; Davison, I. G.; Feliciano, C.; Deisseroth, K.; Augustine, G. J.; Ehlers, M. D.; Feng, G. *Neuron* **2007**, *54*, 205–218.
- Peteanu, L.; Huber, D.; Sobczyk, A.; Svoboda, K. *Nat. Neurosci.* **2007**, *10*, 663–668.
- Wang, H.; Peca, J.; Matsuzaki, M.; Matsuzaki, K.; Noguchi, J.; Qiu, L.; Wang, D.; Zhang, F.; Boyden, E.; Deisseroth, K.; Kasai, H.; Hall, W. C.; Feng, G.; Augustine, G. J. *Proc. Natl. Acad. Sci. U.S.A.* **2007**, *104*, 8143–8148.
- Lima, S. Q.; Miesenböck, G. *Cell* **2005**, *121*, 141–152.
- Schroll, C.; Riemensperger, T.; Bucher, D.; Ehmer, J.; Voller, T.; Erbguth, K.; Gerber, B.; Hendel, T.; Nagel, G.; Buchner, E.; Fiala, A. *Curr. Biol.* **2006**, *16*, 1741–1747.
- Adamantidis, A. R.; Zhang, F.; Aravanis, A. M.; Deisseroth, K.; de Lecea, L. *Nature* **2007**, *450*, 420–424.
- Suh, G. S.; Ben-Tabou de Leon, S.; Tanimoto, H.; Fiala, A.; Benzer, S.; Anderson, D. J. *Curr. Biol.* **2007**, *17*, 905–908.
- Szobota, S.; Gorostiza, P.; Del Bene, F.; Wyatt, C.; Fortin, D. L.; Kolstad, K. D.; Tulyathan, O.; Volgraf, M.; Numano, R.; Aaron, H. L.; Scott, E. K.; Kramer, R. H.; Flannery, J.; Baier, H.; Trauner, D.; Isacoff, E. Y. *Neuron* **2007**, *54*, 535–545.
- Clyne, J. D.; Miesenböck, G. *Cell* **2008**, *133*, 354–363.
- Huber, D.; Peteanu, L.; Ghitani, N.; Ranade, S.; Hromadka, T.; Mainen, Z.; Svoboda, K. *Nature* **2008**, *451*, 61–64.
- Lima, S. Q.; Hromadka, T.; Zador, A. M. Presented at CoSyNe, Salt Lake City, UT, 2008.
- Sulston, J. E.; White, J. G. *Dev. Biol.* **1980**, *78*, 577–597.
- Martin, J. P.; Logsdon, N. *Photochem. Photobiol.* **1987**, *46*, 45–53.
- Miller, J. P.; Selverston, A. *Science* **1979**, *206*, 702–704.
- Garber, S.; Camhi, J. M. *Neuroreport* **1991**, *2*, 181–184.
- Kemenes, G.; Daykin, K.; Elliott, C. J. *J. Neurosci. Methods* **1991**, *39*, 207–216.
- Marder, E. *J. Exp. Biol.* **1984**, *112*, 147–167.
- Kemenes, G. *Gen. Pharmacol.* **1997**, *29*, 7–15.
- Nirenberg, S.; Cepko, C. J. *Neurosci.* **1993**, *13*, 3238–3251.
- Nirenberg, S.; Meister, M. *Neuron* **1997**, *18*, 637–650.
- Sinclair, J. R.; Jacobs, A. L.; Nirenberg, S. *J. Neurosci.* **2004**, *24*, 1459–1467.
- Gao, W.; Xing, B.; Tsien, R. Y.; Rao, J. J. *Am. Chem. Soc.* **2003**, *125*, 11146–11147.
- Wildt, S.; Deuschle, U. *Nat. Biotechnol.* **1999**, *17*, 1175–1178.
- Feliciano, J.; Liu, Y.; Daunert, S. *Biotechnol. Bioeng.* **2006**, *93*, 989–997.
- Stummer, W.; Stocker, S.; Novotny, A.; Heilmann, A.; Sauer, O.; Kempfski, O.; Plesnila, N.; Wietzorek, J.; Reulen, H. J. *J. Photochem. Photobiol. B* **1998**, *45*, 160–169.
- Jay, D. G. *Proc. Natl. Acad. Sci. U.S.A.* **1988**, *85*, 5454–5458.
- Linden, K. G.; Liao, J. C.; Jay, D. G. *Biophys. J.* **1992**, *61*, 956–962.
- Surrey, T.; Elowitz, M. B.; Wolf, P. E.; Yang, F.; Nedelec, F.; Shokat, K.; Leibler, S. *Proc. Natl. Acad. Sci. U.S.A.* **1998**, *95*, 4293–4298.
- Beck, S.; Sakurai, T.; Eustace, B. K.; Beste, G.; Schier, R.; Rudert, F.; Jay, D. G. *Proteomics* **2002**, *2*, 247–255.
- Griffin, B. A.; Adams, S. R.; Tsien, R. Y. *Science* **1998**, *281*, 269–272.
- Adams, S. R.; Campbell, R. E.; Gross, L. A.; Martin, B. R.; Walkup, G. K.; Yao, Y.; Llopis, J.; Tsien, R. Y. *J. Am. Chem. Soc.* **2002**, *124*, 6063–6076.
- Marek, K. W.; Davis, G. W. *Neuron* **2002**, *36*, 805–813.
- Martin, B. R.; Giepmans, B. N.; Adams, S. R.; Tsien, R. Y. *Nat. Biotechnol.* **2005**, *23*, 1308–1314.
- Tour, O.; Meijer, R. M.; Zacharias, D. A.; Adams, S. R.; Tsien, R. Y. *Nat. Biotechnol.* **2003**, *21*, 1505–1508.
- Zhang, C.; Sriratanana, A.; Minamikawa, T.; Nagley, P. *Biochem. Biophys. Res. Commun.* **1998**, *242*, 390–395.
- Bulina, M. E.; Chudakov, D. M.; Britanova, O. V.; Yanushevich, Y. G.; Staroverov, D. B.; Chepurnykh, T. V.; Merzlyak, E. M.; Shkrob, M. A.; Lukyanov, S.; Lukyanov, K. A. *Nat. Biotechnol.* **2006**, *24*, 95–99.
- Bulina, M. E.; Lukyanov, K. A.; Britanova, O. V.; Onichtchouk, D.; Lukyanov, S.; Chudakov, D. M. *Nat. Protoc.* **2006**, *1*, 947–953.
- Baranano, D. E.; Rao, M.; Ferris, C. D.; Snyder, S. H. *Proc. Natl. Acad. Sci. U.S.A.* **2002**, *99*, 16093–16098.

- (55) Sahoo, S. K.; Sawa, T.; Fang, J.; Tanaka, S.; Miyamoto, Y.; Akaike, T.; Maeda, H. *Bioconjugate Chem.* **2002**, *13*, 1031–1038.
- (56) Destexhe, A.; Rudolph, M.; Fellous, J. M.; Sejnowski, T. J. *Neuroscience* **2001**, *107*, 13–24.
- (57) Destexhe, A.; Rudolph, M.; Pare, D. *Nat. Rev. Neurosci.* **2003**, *4*, 739–751.
- (58) Destexhe, A.; Pare, D. *J. Neurophysiol.* **1999**, *81*, 1531–1547.
- (59) Hô, N.; Destexhe, A. *J. Neurophysiol.* **2000**, *84*, 1488–1496.
- (60) Rudolph, M.; Destexhe, A. *Neurocomputing* **2003**, *52*, 907–912.
- (61) Wells, J.; Kao, C.; Jansen, E. D.; Konrad, P.; Mahadevan-Jansen, A. *J. Biomed. Opt.* **2005**, *10*, 064003.
- (62) Wells, J.; Kao, C.; Konrad, P.; Milner, T.; Kim, J.; Mahadevan-Jansen, A.; Jansen, E. D. *Biophys. J.* **2007**, *93*, 2567–2580.
- (63) Voets, T.; Droogmans, G.; Wissenbach, U.; Janssens, A.; Flockerzi, V.; Nilius, B. *Nature* **2004**, *430*, 748–754.
- (64) Fork, R. L. *Science* **1971**, *171*, 907–908.
- (65) Hirase, H.; Nikolenko, V.; Goldberg, J. H.; Yuste, R. *J. Neurobiol.* **2002**, *51*, 237–247.
- (66) Duprat, F.; Guillemare, E.; Romey, G.; Fink, M.; Lesage, F.; Lazdunski, M.; Honore, E. *Proc. Natl. Acad. Sci. U.S.A.* **1995**, *92*, 11796–11800.
- (67) Kourie, J. I. *Am. J. Physiol.* **1998**, *275*, C1–C24.
- (68) Farber, I. C.; Grinvald, A. *Science* **1983**, *222*, 1025–1027.
- (69) Callaway, E. M.; Katz, L. C. *Proc. Natl. Acad. Sci. U.S.A.* **1993**, *90*, 7661–7665.
- (70) Katz, L. C.; Dalva, M. B. *J. Neurosci. Methods* **1994**, *54*, 205–218.
- (71) Walker, J. W.; McCray, J. A.; Hess, G. P. *Biochemistry* **1986**, *25*, 1799–1805.
- (72) Milburn, T.; Matsubara, N.; Billington, A. P.; Udgaonkar, J. B.; Walker, J. W.; Carpenter, B. K.; Webb, W. W.; Marque, J.; Denk, W.; McCray, J. A.; Hess, G. P. *Biochemistry* **1989**, *28*, 49–55.
- (73) Wieboldt, R.; Gee, K. R.; Niu, L.; Ramesh, D.; Carpenter, B. K.; Hess, G. P. *Proc. Natl. Acad. Sci. U.S.A.* **1994**, *91*, 8752–8756.
- (74) Dodt, H. U.; Frick, A.; Kampe, K.; Ziegler, W. *Eur. J. Neurosci.* **1998**, *10*, 3351–3357.
- (75) Kandler, K.; Katz, L. C.; Kauer, J. A. *Nat. Neurosci.* **1998**, *1*, 119–123.
- (76) Schiller, J.; Schiller, Y.; Clapham, D. E. *Nat. Neurosci.* **1998**, *1*, 114–118.
- (77) Dalva, M. B.; Katz, L. C. *Science* **1994**, *265*, 255–258.
- (78) Dantzker, J. L.; Callaway, E. M. *Nat. Neurosci.* **2000**, *3*, 701–707.
- (79) Schubert, D.; Staiger, J. F.; Cho, N.; Kotter, R.; Zilles, K.; Luhmann, H. J. *J. Neurosci.* **2001**, *21*, 3580–3592.
- (80) Shepherd, G. M.; Pologruto, T. A.; Svoboda, K. *Neuron* **2003**, *38*, 277–289.
- (81) Yoshimura, Y.; Callaway, E. M. *Nat. Neurosci.* **2005**, *8*, 1552–1559.
- (82) Yoshimura, Y.; Dantzker, J. L.; Callaway, E. M. *Nature* **2005**, *433*, 868–873.
- (83) Adams, S. R.; Tsien, R. Y. *Annu. Rev. Physiol.* **1993**, *55*, 755–784.
- (84) Denk, W. *Proc. Natl. Acad. Sci. U.S.A.* **1994**, *91*, 6629–6633.
- (85) Pettit, D. L.; Wang, S. S.; Gee, K. R.; Augustine, G. J. *Neuron* **1997**, *19*, 465–471.
- (86) Wang, S. S.; Khiroug, L.; Augustine, G. J. *Proc. Natl. Acad. Sci. U.S.A.* **2000**, *97*, 8635–8640.
- (87) Canepari, M.; Nelson, L.; Papageorgiou, G.; Corrie, J. E.; Ogden, D. J. *J. Neurosci. Methods* **2001**, *112*, 29–42.
- (88) Matsuzaki, M.; Ellis-Davies, G. C.; Nemoto, T.; Miyashita, Y.; Iino, M.; Kasai, H. *Nat. Neurosci.* **2001**, *4*, 1086–1092.
- (89) Nikolenko, V.; Poskanzer, K. E.; Yuste, R. *Nat. Methods* **2007**, *4*, 943–950.
- (90) Ellis-Davies, G. C.; Matsuzaki, M.; Paukert, M.; Kasai, H.; Bergles, D. E. *J. Neurosci.* **2007**, *27*, 6601–6604.
- (91) Matsuzaki, M.; Ellis-Davies, G. C.; Kasai, H. *J. Neurophysiol.* **2008**, *99*, 1535–1544.
- (92) Molnar, P.; Nadler, J. V. *Eur. J. Pharmacol.* **2000**, *391*, 255–262.
- (93) Pettit, D. L.; Augustine, G. J. *J. Neurophysiol.* **2000**, *84*, 28–38.
- (94) Cürten, B.; Kullmann, P. H.; Bier, M. E.; Kandler, K.; Schmidt, B. F. *Photochem. Photobiol.* **2005**, *81*, 641–648.
- (95) Aujard, I.; Benbrahim, C.; Gouget, M.; Ruel, O.; Baudin, J. B.; Neveu, P.; Jullien, L. *Chemistry* **2006**, *12*, 6865–6879.
- (96) Reddy, G. D.; Saggau, P. *J. Biomed. Opt.* **2005**, *10*, 064038.
- (97) Rozsa, B.; Katona, G.; Vizi, E. S.; Varallyay, Z.; Saghy, A.; Valenta, L.; Maak, P.; Fekete, J.; Banyasz, A.; Szpocs, R. *Appl. Opt.* **2007**, *46*, 1860–1865.
- (98) Henderson, R.; Schertler, G. F. *Philos. Trans. R. Soc. London, Ser. B* **1990**, *326*, 379–e89.
- (99) Wald, G. *Nature* **1968**, *219*, 800–807.
- (100) Panda, S.; Nayak, S. K.; Campo, B.; Walker, J. R.; Hogenesch, J. B.; Jegla, T. *Science* **2005**, *307*, 600–604.
- (101) Melyan, Z.; Tattelin, E. E.; Bellingham, J.; Lucas, R. J.; Hankins, M. W. *Nature* **2005**, *433*, 741–745.
- (102) Qiu, X.; Kumbalasiri, T.; Carlson, S. M.; Wong, K. Y.; Krishna, V.; Provencio, I.; Berson, D. M. *Nature* **2005**, *433*, 745–749.
- (103) Brueggemann, L. I.; Sullivan, J. M. *J. Gen. Physiol.* **2002**, *119*, 593–612.
- (104) O'Brien, P. J.; Muellenberg, C. G. *Biochemistry* **1975**, *14*, 1695–700.
- (105) Sineshchekov, O. A.; Jung, K. H.; Spudich, J. L. *Proc. Natl. Acad. Sci. U.S.A.* **2002**, *99*, 8689–8694.
- (106) Nagel, G.; Szellas, T.; Huhn, W.; Kateriya, S.; Adeishvili, N.; Berthold, P.; Ollig, D.; Hegemann, P.; Bamberg, E. *Proc. Natl. Acad. Sci. U.S.A.* **2003**, *100*, 13940–13945.
- (107) Suzuki, T.; Yamasaki, K.; Fujita, S.; Oda, K.; Iseki, M.; Yoshida, K.; Watanabe, M.; Daiyasu, H.; Toh, H.; Asamizu, E.; Tabata, S.; Miura, K.; Fukuzawa, H.; Nakamura, S.; Takahashi, T. *Biochem. Biophys. Res. Commun.* **2003**, *301*, 711–717.
- (108) Bamann, C.; Kirsch, T.; Nagel, G.; Bamberg, E. *J. Mol. Biol.* **2008**, *375*, 686–694.
- (109) Heginbotham, L.; MacKinnon, R. *Biophys. J.* **1993**, *65*, 2089–2096.
- (110) Nagel, G.; Brauner, M.; Liewald, J. F.; Adeishvili, N.; Bamberg, E.; Gottschalk, A. *Curr. Biol.* **2005**, *15*, 2279–2284.
- (111) Gradinaru, V.; Thompson, K. R.; Zhang, F.; Mogri, M.; Kay, K.; Schneider, M. B.; Deisseroth, K. *J. Neurosci.* **2007**, *27*, 14231–14238.
- (112) Bi, A.; Cui, J.; Ma, Y. P.; Olshevskaya, E.; Pu, M.; Dizhoor, A. M.; Pan, Z. H. *Neuron* **2006**, *50*, 23–33.
- (113) Otmakhov, N.; Shirke, A. M.; Malinow, R. *Neuron* **1993**, *10*, 1101–1111.
- (114) Gorostiza, P.; Volgraf, M.; Numano, R.; Szobota, S.; Trauner, D.; Isacoff, E. Y. *Proc. Natl. Acad. Sci. U.S.A.* **2007**, *104*, 10865–10870.
- (115) Caterina, M. J.; Schumacher, M. A.; Tominaga, M.; Rosen, T. A.; Levine, J. D.; Julius, D. *Nature* **1997**, *389*, 816–824.
- (116) McKemy, D. D.; Neuhauser, W. M.; Julius, D. *Nature* **2002**, *416*, 52–58.
- (117) Peier, A. M.; Moqrich, A.; Hergarden, A. C.; Reeve, A. J.; Andersson, D. A.; Story, G. M.; Earley, T. J.; Dragoni, I.; McIntyre, P.; Bevan, S.; Patapoutian, A. *Cell* **2002**, *108*, 705–715.
- (118) Zhao, J.; Gover, T. D.; Muralidharan, S.; Auston, D. A.; Weinreich, D.; Kao, J. P. *Biochemistry* **2006**, *45*, 4915–4926.
- (119) Gilbert, D.; Funk, K.; Dekowski, B.; Lechler, R.; Keller, S.; Mohrlen, F.; Frings, S.; Hagen, V. *ChemBioChem* **2007**, *8*, 89–97.
- (120) Mezey, E.; Toth, Z. E.; Cortright, D. N.; Arzubi, M. K.; Krause, J. E.; Elde, R.; Guo, A.; Blumberg, P. M.; Szallasi, A. *Proc. Natl. Acad. Sci. U.S.A.* **2000**, *97*, 3655–3660.
- (121) Arenkiel, B. R.; Klein, M. E.; Davison, I. G.; Katz, L. C.; Ehlers, M. D. *Nat. Methods* **2008**, *5*, 299–302.
- (122) Brake, A. J.; Wagenbach, M. J.; Julius, D. *Nature* **1994**, *371*, 519–523.
- (123) Valera, S.; Hussy, N.; Evans, R. J.; Adami, N.; North, R. A.; Surprenant, A.; Buell, G. *Nature* **1994**, *371*, 516–519.
- (124) Kaplan, J. H.; Forbush, B.; Hoffman, J. F. *Biochemistry* **1978**, *17*, 1929–1935.
- (125) McCray, J. A.; Trentham, D. R. *Annu. Rev. Biophys. Biophys. Chem.* **1989**, *18*, 239–270.
- (126) Ding, S.; Sachs, F. *J. Gen. Physiol.* **1999**, *113*, 695–720.
- (127) Dowdall, M. J.; Boyne, A. F.; Whittaker, V. P. *Biochem. J.* **1974**, *140*, 1–12.
- (128) Isacoff, E. Y.; Jan, Y. N.; Jan, L. Y. *Nature* **1990**, *345*, 530–534.
- (129) Kobertz, W. R.; Miller, C. *Nat. Struct. Biol.* **1999**, *6*, 1122–1125.
- (130) Sutherland, M. L.; Williams, S. H.; Abedi, R.; Overbeek, P. A.; Pfaffinger, P. J.; Noebels, J. L. *Proc. Natl. Acad. Sci. U.S.A.* **1999**, *96*, 2451–2455.
- (131) Nadeau, H.; McKinney, S.; Anderson, D. J.; Lester, H. A. *J. Neurophysiol.* **2000**, *84*, 1062–1075.
- (132) Howe, J. R. *J. Neurophysiol.* **1996**, *76*, 510–519.
- (133) Shannon, C. E. *IEEE Trans. Inf. Theory* **1956**, *2*, 3.

CR078221B